

GT2013-94656

AERODYNAMIC ANALYSIS OF A BOUNDARY-LAYER-INGESTING DISTORTION-TOLERANT FAN

Razvan V. Florea, Dmytro Voytovych, Gregory Tillman, Mark Stucky, Aamir Shabbir, Om Sharma,

United Technologies Research Center, East Hartford, CT, USA

and

David J. Arend

NASA Glenn Research Center at Lewis Field, OH, USA

ABSTRACT

The paper describes the aerodynamic CFD analysis that was conducted to address the integration of an embedded-engine (EE) inlet with the fan stage. A highly airframe-integrated, distortion-tolerant propulsion preliminary design study was carried out to quantify fuel burn benefits associated with boundary layer ingestion (BLI) for “N+2” blended wing body (BWB) concepts. The study indicated that low-loss inlets and high-performance, distortion-tolerant turbomachines are key technologies required to achieve a 3-5% BLI fuel burn benefit relative to a baseline high-performance, pylon-mounted, propulsion system. A hierarchical, multi-objective, computational fluid dynamics-based aerodynamic design optimization that combined global and local shaping was carried out to design a high-performance embedded-engine inlet and an associated fan stage. The scaled-down design will be manufactured and tested in NASA’s 8’x6’ Transonic Wind Tunnel. Unsteady calculations were performed for the coupled inlet and fan rotor and inlet, fan rotor and exit guide vanes. The calculations show that the BLI distortion propagates through the fan largely un-attenuated. The impact of distortion on the unsteady blade loading, fan rotor and fan stage efficiency and pressure ratio is analyzed. The fan stage pressure ratio is provided as a time-averaged and full-wheel circumferential-averaged value. Computational analyses were performed to validate the system study and design-phase predictions in terms of fan stage performance and operability. For example, fan stage efficiency losses are less than 0.5-1.5% when compared to a fan stage in clean flow. In addition, these calculations will be used to provide pretest predictions and guidance for risk mitigation for the wind tunnel test.

INTRODUCTION

The performance objectives for NASA’s Generation-After Next (N+2) BWB aircraft research require dramatic reductions in noise, emissions, and fuel burn relative to conventional aircraft ([1]). A concept that holds promise for meeting these objectives is boundary layer ingestion into the propulsion system. However, the large flow distortions lead to strong coupling between the fan and upstream flow fields. The challenge lays then on to the propulsion system where the high inlet flow distortion drives performance, aeromechanical, stability/operability and acoustic issues within the compression system. The impact of the compromises in engine performance required to overcome these issues is a key question that must be addressed.

In recent years, a number of system-level studies of advanced aircraft with BLI propulsion have been carried out and a recent thorough review was done by Hardin et al. [2]. Some of the benefits of BLI propulsion are reviewed by Plas et al. [3], who describe maximum propulsive efficiency benefits of up to 28%. Actual achievable benefits are a function of several elements, such as the amount of airframe boundary layer that can be ingested; wake properties; the engine cycle; composition of the overall airframe drag; and losses incurred in the inlet and turbomachinery due to boundary layer ingestion and engine operation in the presence of distortion. The study estimates that for the specific vehicle system and mission a net fuel burn reduction of between 3 and 4% should be achievable with a modest level of boundary layer ingestion (up to 16%) after properly accounting for reductions in engine performance.

SYSTEM ANALYSIS AND INLET DESIGN

The overall goal of the BLI-EE research was to develop a distortion-tolerant inlet-fan propulsor system design that

*Currently at Pratt & Whitney, East Hartford, CT, USA.

This work is in part a work of the U.S. Government. ASME disclaims all interest in the U.S. Government's contributions.

simultaneously targets less than 2% reduction in fan efficiency and less than 2% reduction in stability margin relative to a clean-inflow baseline. In order to identify BLI propulsion concepts with the most promise for providing system-level benefits, Hardin et al. [2] conducted a highly airframe-integrated, distortion-tolerant propulsion preliminary design study. Fuel burn benefits associated with BLI for BWB concepts were identified. First, for a given BWB reference vehicle, a high-level, propulsion-system system study was performed to evaluate optimal Ultra-High-Bypass (UHB) engine architecture configurations. The study used the external flow field of the Boeing N2A-ExTE hybrid wing body aircraft, including its boundary layer profile. The aircraft is an advanced, BWB design for podded or BLI propulsion, with an extended trailing edge aimed at providing additional aft acoustic shielding of jet noise (Kawai et al. [4]). The design cruise Mach number was 0.8 at an altitude of 35,000 feet. The isentropic Mach number contours on the suction side at cruise conditions are shown in Figure 1. The percentage of the total viscous drag that can be ingested by propulsion systems embedded on the suction side of the reference vehicle aft of the wings is limited to around 12% or less. The reference vehicle is configured with two podded larger diameter propulsion systems that do not ingest any boundary layer air. The reference propulsion system for the current study was chosen as UHB turbofan, with a reference cycle chosen to have a bypass ratio of 16 and a fan pressure ratio of 1.35. The BLI-EE system study attempted to capture the vehicle impacts associated with changes in propulsion system drag, and to a lesser extent weight, where these changes can be estimated. Propulsion system performance changes due to BLI operation were to be included as well. Use of the same airframe and engine cycle for both podded and BLI configurations was intended to give a more accurate evaluation of the benefits of the BLI concept exclusive of any benefits due to airframe or engine features other than BLI.

Results of the preliminary study indicated that the engines should be located relatively far aft, and distributed across the middle portion of the airframe to capture the entire spanwise extent of the boundary layer available at the engine location. For the specific reference vehicle, this requirement translated to a five-engine architecture of relatively smaller diameter than the two podded larger diameter engines of the reference configuration. The study further indicated that low-loss inlets and high-performance, distortion-tolerant turbomachines are key technologies required to achieve a 3-5% BLI fuel burn benefit for N+2 aircraft relative to a baseline high-performance, pylon-mounted, propulsion system. Next, a hierarchical, multi-objective, computational fluid dynamics-based aerodynamic design optimization that combined global and local shaping was carried out by Florea et al. [5] to design a high-performance EE inlet and an associated fan stage. The CFD inlet design initially identified short inlets with length/diameter of 0.6 and limited total pressure losses. The resulting inlets were further optimized for minimum distortion content in the first three harmonics. A

three-dimensional view of the final UTRC inlet design along with the wall pressure distribution (normalized by the total pressure upstream of the inlet lip) and Mach number at the aerodynamic interface plane (AIP) at nominal inlet conditions are shown in Figure 2. Also shown is the total pressure field at AIP.

Note that the initial UTRC system study assumed a particular correlation between the inlet aspect ratio and the inlet length. The CFD inlet design led to shorter inlets satisfying the system study requirements, and resulting in a 3-5% BLI fuel burn benefit for the N+2 aircraft relative to a baseline high-performance, pylon-mounted, propulsion system. Also, one of the benefits of shorter inlets is that the boundary layer does not have the length to develop and penetrate significantly into the core region.

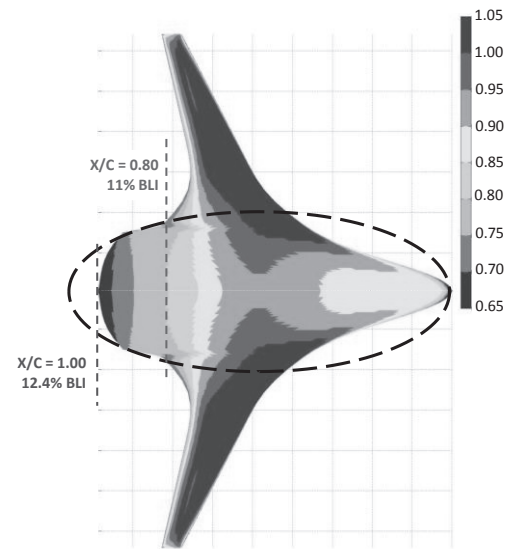


Figure 1. Suction side isentropic Mach number contours. BLI benefit limited by viscous drag accessible on N+2 vehicle upper surface (~12% or less depending on inlet location). Solution from Boeing, (Kawai et al. [4]).

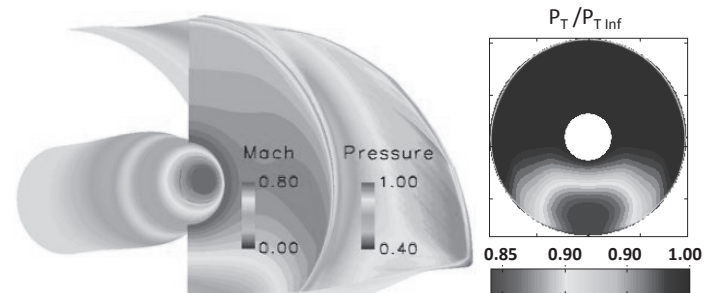


Figure 2. a) Three-dimensional view of the UTRC inlet along with the wall pressure distribution (normalized by the total pressure upstream of the inlet lip) and Mach number at AIP at nominal conditions. **b)** Total pressure field at AIP (Florea et al. [5]).

From inlet design perspective, the five-engine architecture translates into a multiple (five) inlet (MI) configuration with no space in-between. Each inlet is distinct except near the BWB where adjacent inlets come together with a common lip. However, for the purpose of testing, a scaled-down design in single-inlet configuration will be manufactured and tested in a NASA wind tunnel. A large-scale 8'x6' Transonic Wind Tunnel (TWT) test of a multi-use, BLI distortion-tolerant propulsor experiment has been defined by Arend et al. [7], and will initially focus on aircraft cruise operating conditions. It consists of a single boundary layer ingesting inlet coupled with a 22" diameter distortion-tolerant fan stage mounted into raised wind tunnel floor special test equipment designed to simulate the upper aft surface of a hybrid wing body aircraft. As shown in Figure 3, this experiment is designed to ingest the naturally developed wind tunnel floor boundary layer regulated by a dedicated boundary layer bleed system. The experiment is to be powered by NASA's Ultra-High Bypass (UHB) fan drive rig.

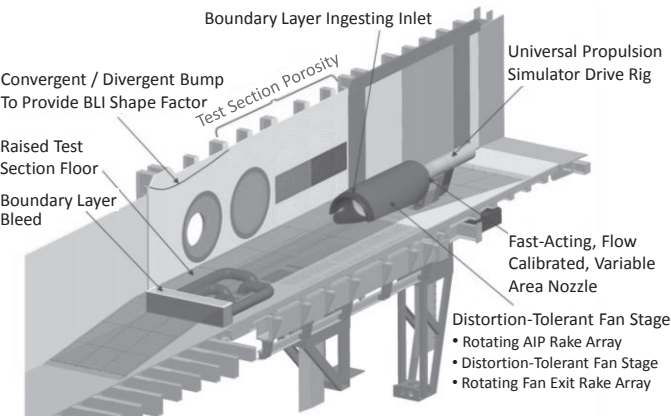


Figure 3. Robust Design Boundary Layer Ingesting Propulsor Experiment Layout (Arend et al. [7]).

INLET-FAN COUPLING

The next level of aerodynamic CFD analysis was conducted to address the integration of the embedded-engine inlet with the fan stage. For the final inlet design, UTRC performed high fidelity steady and unsteady fluid-flow calculations starting with the fan in clean and distorted (loosely coupled) in-flow and ending with the fully coupled inlet/fan stage with in-flow distortion prescribed at the inlet throat as defined by the inlet calculations. Specifically, during the inlet aerodynamic design and analysis step, to accurately capture the flow distortion profiles at throat location and within the inlet, the computational domain was enlarged to include the inlet lip and upstream BWB domain and flow conditions. The fan was not included. However, downstream of the AIP, the flowpath was extended and modified and static pressure boundary conditions were imposed to get the desired mass flow and transonic conditions at fan location. The resulting total pressure, total temperature and flow angles profiles at throat location

were used during the inlet-fan coupling analysis. The inlet-fan calculations were done using UTRC/PW state of the art turbomachinery RANS aerodynamic code based on the Ni's scheme and using dual time step and $k\omega$ turbulence model.

The configuration defined by the coupled inlet / fan / EGV is shown in Figure 4. Fan efficiency and aerodynamic blade loading were evaluated. Some of the aerodynamic results for the fan alone are summarized in Figure 5. The fan maximum efficiency with clean in-flow is around 96.5%. The coupled UTRC inlet / fan unsteady calculations show about 0.5% or less drop in maximum fan efficiency and about 7% drop in corresponding mass flow when compared to clean in-flow. In addition, the maximum fan stage efficiency (EGV included) in the presence of distortion (UTRC inlet) is around 95.2%. For the steady calculations with clean flow the steady adiabatic efficiency is based on fan-passage mass-averaged quantities. For the unsteady calculations, the fan stage adiabatic efficiency is based on time-averaged and full-wheel mass-averaged values.

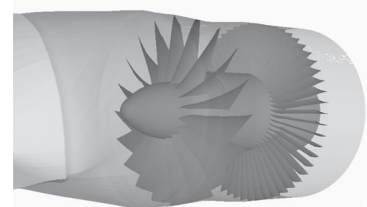


Figure 4. Inlet/UHB turbofan, with bypass ratio of 16 and a fan pressure ratio of 1.35.

Also shown in Figure 5, is the drop in efficiency for a highly embedded engine configuration, NASA "Inlet A", with a length/diameter ratio of 3 (Berrier et al. [6]). This validates the impact of inlet design and inlet-fan coupling on overall distortion-tolerant propulsion system design. Specifically, during the inlet design step, the UTRC inlet was optimized for minimum distortion content in the first three harmonics and limited total pressure losses. As a result the distortion is "squeezed" towards the fan outer diameter wall. In the region where the flow is clean, the mass flow is limited by the transonic conditions near the tip. Only a slight increase in Mach number is observed with only a small reduction in adiabatic efficiency. In the distortion region, defined primarily by reduced total pressure and momentum conditions, we see a reduction in mass flow, hence the net effect of 7% drop in corresponding mass flow through the fan and a limited impact on adiabatic efficiency.

For the coupled BWB / inlet calculations, the distortion is captured at the inlet throat, develops through the inlet and provides the pattern shown in Figure 2 (at AIP in the absence of the fan). The AIP is defined here about 0.4 chords upstream of the fan. When the inlet is coupled with fan, the fan itself provides a rotational effect on the distortion. However, the distortion propagates through the fan with little or no mixing at all. Shown in Figure 6 is the distortion presented as mass flow deficit at the AIP, which enters the fan, and immediately

downstream of the fan. The radial profile for the pitch-averaged maximum mass flow passage is computed first and then used for the mass flow deficit calculation.

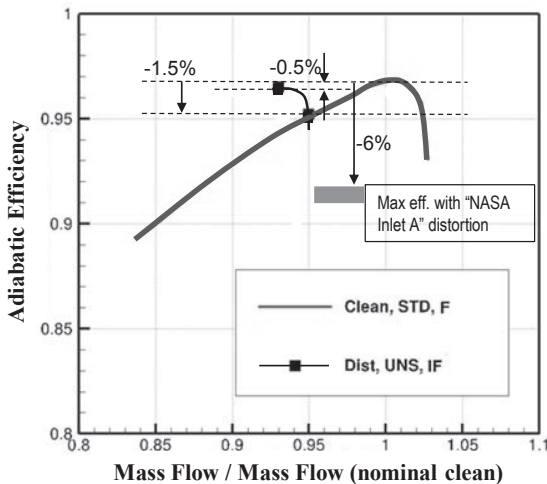


Figure 5. RANS calculations with clean flow for steady fan alone (Clean, STD, F) and with distortion at inlet throat for unsteady UTRC inlet/full wheel fan (DIST, UNS, IF) (Florea et al. [5]).

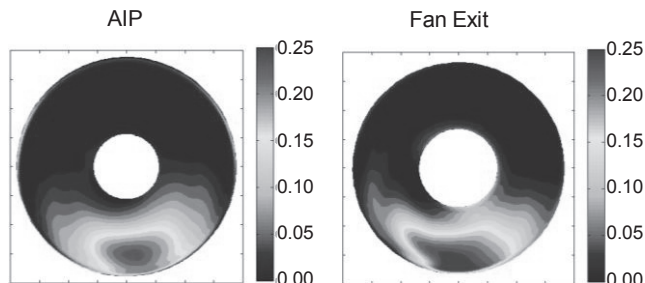


Figure 6. Mass flow deficit (w.r.t. pitch-averaged maximum flow).

A critical aspect of the transition from the multiple-inlet flight configuration to the single-inlet test article is to quantify the similarities between the distortion patterns upstream at the AIP. Shown in Figure 7 and Figure 8 are the total pressure harmonic content (Euclidian norm) and radial profiles for the two configurations. While the harmonic content spectrums for the two configurations are very close, some differences in radial profile for the first and third harmonics are seen, with higher loading in the first harmonic towards the tip for the single-inlet configuration. A small increase in mean (time-averaged) and unsteady tip loading corresponding to the first harmonic is expected for the single-inlet test article with potential limitations on the blade aeromechanics. Shown in Figure 9 are the time-averaged isentropic Mach number contours on blade pressure and suction side surfaces for the multiple and single-inlet configurations. As a result, the previous aeromechanical

analysis performed by Bakhle et al. [8] for the 76" fan in multiple-inlet configuration distortion will be extended to the 22" fan test article with the new blade loadings associated with the wind tunnel conditions.

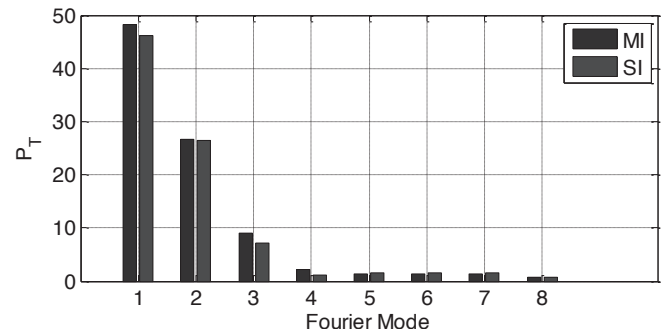


Figure 7. Comparison of total pressure harmonic content for multiple-inlet (MI) vs. single-inlet (SI) configurations.

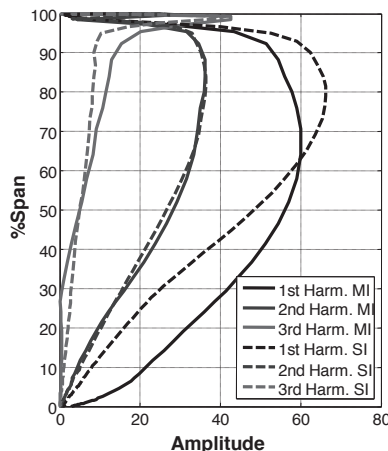


Figure 8. Comparison of total pressure harmonic profiles for multiple-inlet (MI) vs. single-inlet (SI) configurations.

INLET-FAN-EGV (WIND TUNNEL CONFIGURATION)

To reduce costs, and simplify the design and operation of the distortion-tolerant propulsor experiment, the core was eliminated and the EGV and duct were redesigned (Figure 10) to accommodate for the distortion downstream of the fan. In addition, the 22" fan root was strengthened. Pre-test predictions were carried out to evaluate inlet/fan/EGV performance for the wind tunnel configuration with the UTRC inlet in single mode configuration. The computational domain for these calculations starts at inlet throat and ends downstream of the EGV. As will be discussed further on, such a domain seems to be sufficient for performance evaluations.

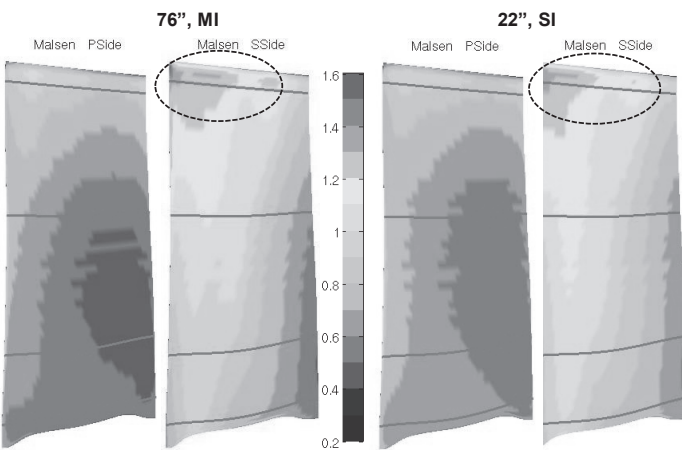


Figure 9. Blade loading comparison for multiple-inlet vs. single-inlet configurations: Time-average isentropic Mach number contours on the pressure side (PSide) and suction side (SSide).

Shown in Figure 11 and Figure 12 are the total pressure ratio and efficiency for the fan only and the fan stage (with EGV). Note that there is about 1.4% drop in maximum efficiency when compared with 76" multiple inlet fan configuration. Effects responsible for this drop include the decrease in Reynolds number, the change in blade loading due to the distortion profile associated with single inlet configuration, the change in root definition due to the fan root blade strengthened and the elimination of the core. Each of these effects is relatively small, corresponding to around 0.3 to 0.4% drop in efficiency. When compared with a typical fan performance map in the absence of distortion (Figure 5), the BLI-inlet/fan configuration allows the excursion towards maximum mass flow (choke point) to be less steep. Specifically, as the mass flow through the fan is increased, and more fan passages are choked, the distortion in the inlet upstream of the fan is squeezed down, allowing for more flow through the fan, leading also to additional inlet losses. However, when the mass flow is decreased and the fan moves towards stall, the distortion through the inlet grows, leading to additional fan leading edge incidence. Shown in Figure 13 are the Mach number flow fields at the AIP and through the fan passage at 61% span for two different flow conditions (single inlet configuration).

At lower mass flows (towards stall), unsteadiness at the inlet throat section is observed. That seems to indicate that for lower mass flow (below corrected mass flow of 100 lb/s), the computational domain has to be increased upstream to capture a portion of the wind tunnel configuration.

Figure 14 shows the total pressure ratio excursions for different passages as a function of the corrected mass flow through each passage. Three sets of conditions are considered identified as nominal, 1 and 2, and defined by the average conditions on the total pressure ratio map shown in Figure 11. Point 1 is close to choked conditions, and point 2 is before

nominal, towards stall. Each dotted portion of the curve refers to the fan passages in the top undistorted portion of the flow. The continuous line refers to the fan passages passing through the BLI distortion at the bottom. The quantity $\Delta W_C = 14.7\%$ defines the corrected mass flow excursion for each individual flow passage at nominal distortion conditions. Towards choked conditions (1), the corrected mass flow excursion decreases to 14.4% and towards stall (2) increases to 15.8. Note that for NASA inlet A, at nominal conditions, the corrected mass flow excursion is about 23%. To a first approximation, the extent of these excursions is a measure of the stability margin, increased in our case when UTRC inlet design is compared with NASA inlet A.

Shown in Figure 15 are the time-averaged Mach number contours for the flow through the EGV at several axial and radial locations. Specifically, the flow shows significant distortion content as it exits the fan upstream of the EGV. As the flow propagates through the EGV, shown here at three radial locations and downstream of the EGV, the distortion is gradually reduced.

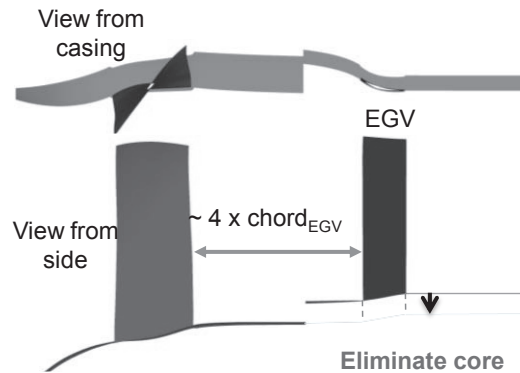


Figure 10. Schematic view of the original fan and EGV with core (BWB configuration). Core is marked for elimination in test article mode.

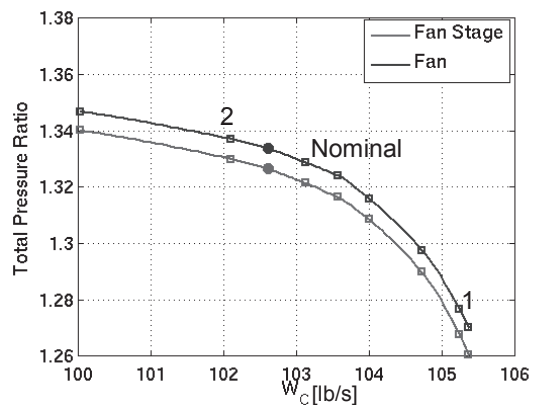


Figure 11. Total pressure ratio for the 22" fan and fan stage (EGV) coupled with the UTRC inlet (single inlet distortion).

CONCLUSIONS

A high-level, trade-factor-based system study has identified a low-loss inlet and high-performance, distortion-tolerant turbomachinery as key technologies consistent with achieving net system level benefits. A coupled inlet, fan and EGV final aerodynamic analysis shows that the fan performance target, measured relative to a technology-upgraded baseline fan, is achieved. The calculations show that the BLI distortion propagates through the fan largely un-attenuated. As the flow propagates through the EGV, the distortion is gradually reduced.

The present CFD inlet/fan analysis will be used as a pretest prediction and guidance for risk mitigation for the wind tunnel test. The single-inlet test article and the multiple-inlet flight configuration show similar distortion patterns upstream at the AIP. Scaling to the 22 in. rig wind tunnel dimensions & operating conditions results in the preservation of the performance benefits. The future test will be used to validate the fan performance and the overall 3-5% BLI fuel burn benefit predicted by the system study for the N+2 aircraft relative to a baseline high-performance, pylon-mounted, propulsion system.

ACKNOWLEDGMENTS

This work was funded under NASA Contract NNC07CB59C, Robust Design for Embedded Engine Systems (RDEES), Phase 2 with Mr. David Arend as Technical Monitor. The authors are grateful to Dr. Bill Cousins for his insight into the fan stability and operability.

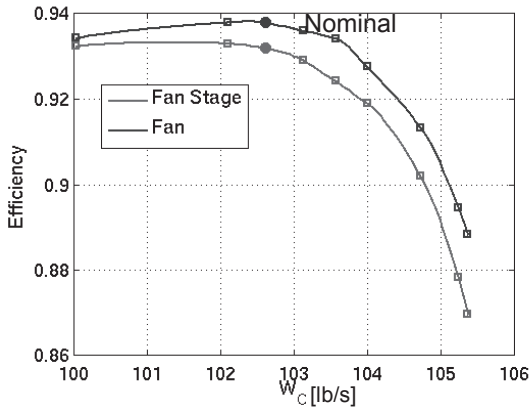


Figure 12. Efficiency for the 22" fan and fan stage (EGV) coupled with the UTRC inlet (single inlet distortion).

REFERENCES

- [1] Amendment No. 4 to the NASA Research Announcement (NRA) Entitled "Research Opportunities in Aeronautics—2006 (ROA-2006)," NNH06ZEA001N, Release May 23, 2006.
- [2] Hardin, L. H., Tillman, T. G., Sharma, O. P., Berton, J., and Arend, D. J., "Aircraft System Study of Boundary

Layer Ingesting Propulsion," AIAA 2012-3993, presented at the 48th AIAA/ASME/SAE/ASEE Joint Propulsion Conference & Exhibit, Jul 30- Aug 1, 2012.

- [3] Plas, A.E., Sargeant, M.A., Madani, V., Crichton, D., Greitzer, E.M., Hynes, T. P., and Hall C.A. "Performance of a Boundary Layer Ingesting (BLI) Propulsion System," 45th AIAA Aerospace Sciences Meeting, AIAA 2007-450, January 2007.
- [4] Kawai, R. T., Friedman, D. L., and Serrano, L., *Blended Wing Body (BWB) Boundary Layer Ingestion (BLI) Inlet Configuration and System Studies*. NASA CR-2006-214534, December 2006.
- [5] Florea R.V., Matalanis, C., Hardin, L.W., Stucky, M., and Aamir Shabbir, A., "Parametric Analysis and Design for Embedded Engine Inlets," AIAA 2012-3994, presented at the 48th AIAA/ASME/SAE/ASEE Joint Propulsion Conference & Exhibit, Jul 30- Aug 1, 2012.
- [6] Berrier, Bobby L., Carter, Melissa B., and Allan, Brian G., "High Reynolds Number Investigation of a Flush-Mounted, S-Duct Inlet with Large Amounts of Boundary Layer Ingestion," NASA/TP-2005-213766.
- [7] Arend, D., Tillman, G.T., and O'Brien W.F., "Generation After Next Propulsor Research: Robust Design for Embedded Engine Systems," AIAA 2012-4041, presented at the 48th AIAA/ASME/SAE/ASEE Joint Propulsion Conference & Exhibit, Jul 30- Aug 1, 2012.
- [8] Bakhle, M.A., Reddy, T.S.R., Herrick, G.P., Shabbir, A., and Florea, R.V., "Aeromechanics Analysis of a Boundary Layer Ingesting Fan," AIAA 2012-3995, presented at the 48th AIAA/ASME/SAE/ASEE Joint Propulsion Conference & Exhibit, Jul 30- Aug 1, 2012.

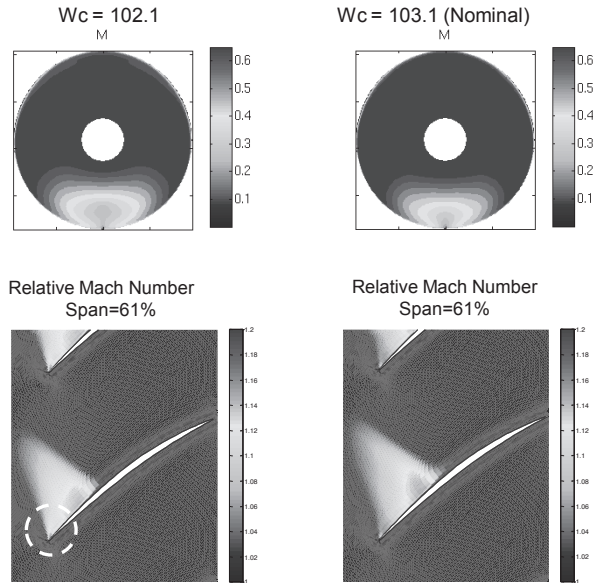


Figure 13. Mach number flow fields at AIP and through the fan passage at 61% span for two different flow conditions (single inlet configuration).

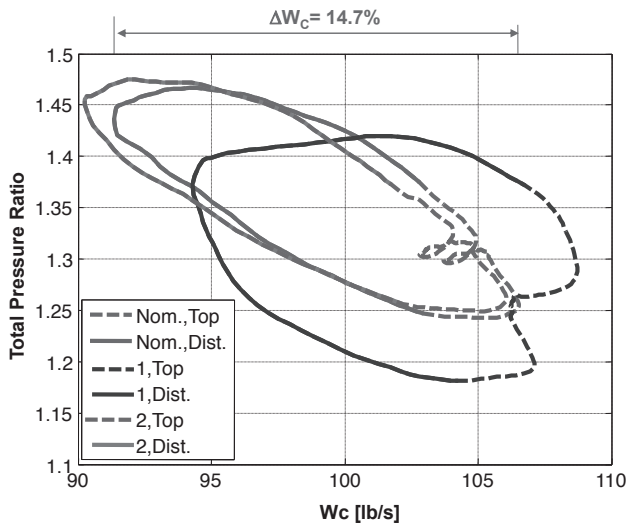


Figure 14. Total pressure ratio excursions for 3 sets of conditions: nominal, near choked (1), towards stall (2)

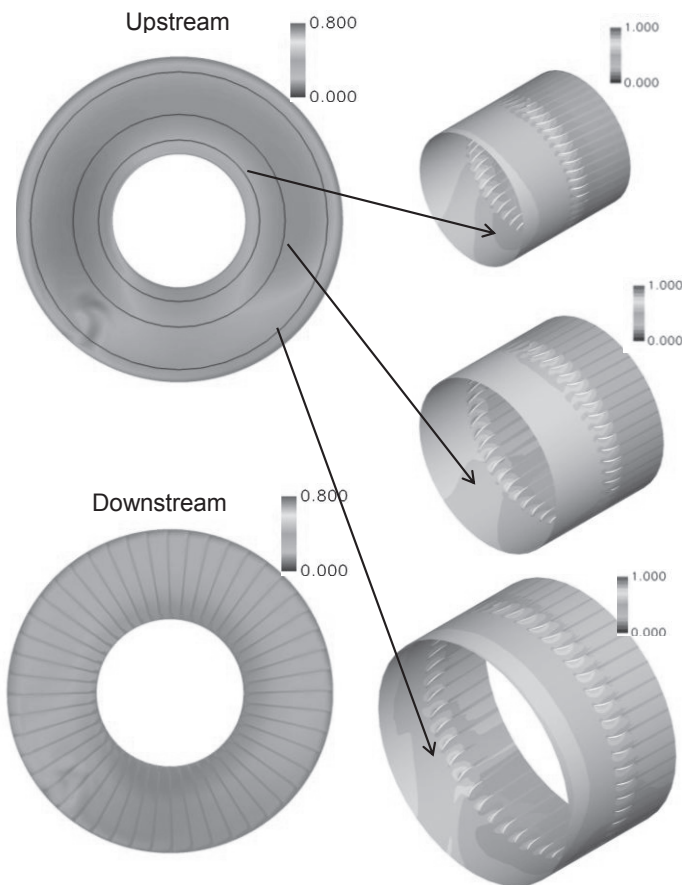


Figure 15. Time-averaged Mach number contours for the flow through the EGV at several axial and radial locations. (22" fan, single inlet configuration).